Relative stability of columnar and crystalline phases in a system of parallel hard spherocylinders

J. A. C. Veerman and D. Frenkel

FOM−Institute for Atomic and Molecular Physics, Kruislaan 407, 1098 SJ Amsterdam, The Netherlands
(Received 2 November 1990)

We report a computer-simulation study of the stability of the columnar phase in a system of parallel spherocylinders with aspect ratios $L/D = 5$ and ∞. It is found that the range of stability of the columnar phase is strongly dependent upon the system size. In particular, for particles with an aspect ratio $L/D = 5$, the columnar phase that is observed in small systems ($N = 90$) disappears for a system of $N = 1080$ particles. In its place, a simple hexagonal crystal ("AAA stacking") appears. On the basis of our present simulations, we cannot tell whether the latter phase is truly crystalline or possibly a smectic-B phase. For particles with an aspect ratio $L/D = \infty$, similar behavior is observed, although in this case a stable columnar "pocket" remains, even for the largest systems we studied. We have computed the locations of all phase transitions involving the new hexagonal phase.

I. INTRODUCTION

The molecules that constitute liquid-crystalline materials are often quite complex. Yet it appears that non-spherical hard-core interparticle interactions are all that is needed to explain the occurrence of a number of liquid-crystalline phases. Liquid-crystalline phases have been found by computer simulation in various systems of hard-core particles.[1−7] A relatively simple hard-core system in which liquid-crystalline behavior can be observed is the parallel hard-spherocylinder system. According to previous computer calculations[7] this system has a nematic, smectic, and also a columnar phase. The phase diagram of the system, as calculated in Ref. 7, is shown in Fig. 1. In this figure the phases are given as a function of the length-to-width parameter L/D, where L is the length of the cylinder put in between the two hemispheres, and D is the diameter of the cylinder; the "total length" of the spherocylinder is $L+D$. Because of scaling properties, the $L/D = \infty$ system is equivalent to a system of parallel hard (flat) cylinders with finite, but otherwise arbitrary, length L.

In the $L/D = \infty$ system, the simulations of Ref. 7 seemed to indicate that a weakly first-order (or, less likely, continuous) smectic-columnar transition occurred. However, free-energy calculations were not consistent with the observed transition point. Also, it is extremely unlikely that a smectic-A phase would transform continuously into a columnar phase, without going through an intermediate (e.g., solid, smectic-B or nematic) phase. This suggested that the identification of the different phases in Ref. 7 was incorrect or incomplete. Moreover, the systems studied in the computer simulations of Ref. 7 consisted of only 90, or, at most, 270 particles. In such small a system, finite-size effects can easily occur.

The phase behavior of the parallel spherocylinder system was reproduced qualitatively by various theories.[8−14] However, although all theories found evidence for a smectic phase, their predictions concerning the columnar

phase differed: in Ref. 13 a divergence in the structure factor along the parallel direction is observed for $5 \leq L/D \leq 10$, indicating that the columnar phase is unstable with respect to solidlike fluctuations. In Ref. 14 the authors find a stable smectic-A and solid (or smectic-B) phase by direct analysis, but not a stable columnar phase.

The above summary illustrates that evidence for the existence of a stable columnar phase in the parallel spherocylinder system is not as unequivocal as it is for the smectic phase. In the present article we report the results of Monte Carlo (MC) and molecular-dynamics (MD) simulations performed on systems with $L/D = 5$ and ∞. In these simulations we used systems of 1080 particles. A
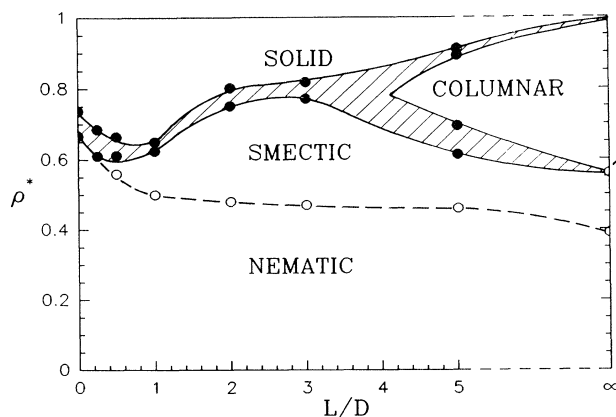

FIG. 1. Phase diagram of the parallel hard-spherocylinder system as given in Ref. 7. The phase diagram was obtained for a system size of 90 particles. The shaded regions correspond to two-phase regions. The question mark indicates that the results concerning the smectic-columnar phase transition are not unambiguous in Ref. 7.

set of "control runs" on a 90-particle system was also performed for the $L/D=5$ system. We will show that in most cases the columnar phase found in the 90-particle system is not stable in the 1080-particle system. Instead, a phase with the columnar hexagonal lattice in the transverse direction, but with a periodic structure in the direction parallel to the molecular axes ("AAA-stacked solid") appears to be stable. The present paper is organized as follows. In Sec. II, we report a study of the system-size dependence of the stability of the columnar phase. In Sec. III, we determine the transition densities of the various phases in the 1080-particle system, and we present a tentative "revised" phase diagram for the parallel spherocylinder system.

II. STABILITY OF THE COLUMNAR PHASE

A. Numerical techniques

We performed a number of runs both for the $L/D=5$ and the $L/D=\infty$ systems. Every series of runs was started from a high-density initial configuration that was constructed to be either crystalline or columnar. These configurations were slowly expanded and equilibrated using constant-stress MC simulations. On the final configurations thus obtained for various densities we carried out a molecular-dynamics simulation to study the time evolution of the system.

The starting configurations for $L/D=5$ were the following.

(i) 90-particle "ABC-stacked" lattice, $\rho^*=0.86$.
(ii) 90-particle columnar configuration, $\rho^*=0.80$.
(iii) 1080-particle ABC-stacked lattice, $\rho^*=0.86$.
(iv) 1080-particle columnar configuration, $\rho^*=0.80$.

For $L/D=\infty$, the starting configurations were the following.

(i) 1080-particle AAA-stacked lattice, $\rho^*=0.86$.
(ii) 1080-particle columnar configuration, $\rho^*=0.90$.

Here ρ^* is the density relative to the close-packed density. By ABC-stacked we mean a lattice in which the particles are stacked in the same way as spherical particles in a fcc lattice. The AAA-stacked lattice, like the ABC-stacked lattice, has fcc-like hexagonal symmetry within the layers perpendicular to the particle alignment, but in contrast to the ABC-stacked structure, where the particle are positioned in the interstitial holes of an adjacent layer, now particles of adjacent layers are directly on top of one another. It is not intuitively obvious that such a crystal structure should be mechanically stable at any density.

The number of layers in the parallel direction was 3 for the 90-particle lattice, and 9 for the 1080-particle lattice. The number of MC cycles performed on a system at a particular density varied from 3000 to 10 000 MC cycles per particle with an acceptance ratio of about 30%. During expansion the density was changed in steps of $\Delta\rho^*=0.02$ to 0.04. The number of collisions in a MD run varied between 400 and 1000 collisions per particle. One MD run took about as much computer time as one MC equilibration run.

B. MC and MD analyses

During the MC runs we identified the structure of the systems by determining the transverse and longitudinal density distribution functions $g_\perp$ and $g_\parallel$, respectively, as well as by taking snapshots of the final configurations. In order to follow the time evolution of the systems during a MD run we measured a number of quantities, which we previously used to study nucleation phenomena in low-L/D systems.[15]

1. Thermal quantity

Compressibility factor. The definition of this quantity is

$$\Pi^* = PV/NkT - 1 \ . \tag{1}$$

Any drift in it indicates that the system is not (yet) in equilibrium. Moreover, the density dependence of Π^* tells us something about the order of a phase transition: When it is first order, the compressibility factor will show a discontinuous jump. When it is higher order there will be no such jump.

2. Dynamical quantity

Mean-square displacement. We measured the diffusion parallel and perpendicular to the alignment of the cylinders by means of the mean-squared displacements parallel and perpendicular to the alignment of the spherocylinders:

$$\langle R_\parallel^2(t) \rangle = N^{-1} \sum_j [r_{\parallel j}(t) - r_{\parallel j}(0)]^2 \tag{2}$$

and

$$\langle R_\perp^2(t) \rangle = N^{-1} \sum_j [r_{\perp j}(t) - r_{\perp j}(0)]^2 \ . \tag{3}$$

When a system is ordered in a certain direction there will be little diffusion in that direction. When the system is fluidlike, the mean-squared displacement will increase linearly in time.

3. Structural quantities

Structure factors. In order to obtain insight into the degree of periodicity within the system we measured the maximum value of the structure factors for wave vectors parallel and perpendicular to the alignment of the cylinders:

$$S_m(\mathbf{k}_\parallel) = \max_{\mathbf{k}_\parallel} N^{-1} \left| \sum_j \exp i\mathbf{k}_\parallel \cdot \mathbf{r}_j \right|^2 \ , \tag{4}$$

$$S_m(\mathbf{k}_\perp) = \max_{\mathbf{k}_\perp} N^{-1} \left| \sum_j \exp i\mathbf{k}_\perp \cdot \mathbf{r}_j \right|^2 \ . \tag{5}$$

When the system has a periodicity corresponding to a certain wave vector, the corresponding structure factor is of $O(N)$. Without such a periodicity the structure factor is of $O(1)$. The maximum value was determined for wave vectors within a certain cutoff. (See the Appendix for details on this.) Due to this cutoff, the behavior of the structure factor is different for the different systems we

studied: In the 90-particle system, $S_m(\mathbf{k}_{\parallel})$ and $S_m(\mathbf{k}_{\perp})$ are large both for the AAA- and for the ABC-stacked lattice. For the 1080-particle system, $S_m(\mathbf{k}_{\parallel})$ is also large for both lattice types. However, $S_m(\mathbf{k}_{\perp})$ is large for the AAA-stacked lattice, but small for the ABC-stacked lattice. The identification of both lattice types is therefore facilitated by the cutoff. The smectic phase can be discerned from the ABC-stacked lattice because of its diffusion in the transverse direction and the small value of ψ_6^2 (see below).

Bond order parameter. We chose the following definition for this quantity:

$$\psi_6^2 = (9N^2)^{-1} \left| {\sum_{i,j}}' \exp 6i\theta_{ij} \right|^2 . \tag{6}$$

In this equation θ_{ij} is defined as angle between the projection of $\mathbf{r}_{ij}$ on the transverse plane and a fixed axis in this plane. The sum is taken over all pairs of particles for which

$$r_{\parallel ij} < 0.7r_{\parallel NN} \ , \quad r_{\perp ij} < 1.35r_{\perp NN} \ . \tag{7}$$

Here $r_{\parallel NN}$ and $r_{\perp NN}$ are the parallel and perpendicular distances between nearest neighbors in a perfect ABC-stacked lattice. The cutoff is chosen in such a way that in a lattice the sum is only taken over nearest neighbors within the same transverse layer. By construction, $\psi_6^2 = 1$ for a perfect lattice. For a completely disordered system, $\psi_6^2 \approx 0$. For a columnar phase, however, $\psi_6^2 > 1$. The reason for this is that in the transverse direction the system is hexagonal (hence there is a "constructive contri-
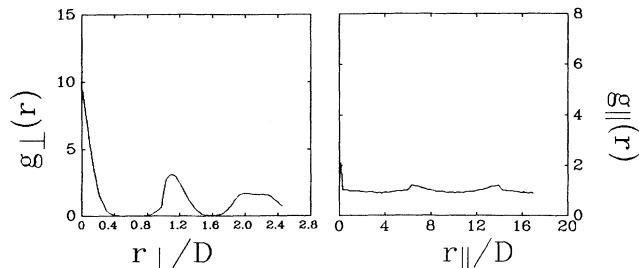

FIG. 3. Same as in Fig. 2 for $L/D = 5$, 90 particles at a density $\rho^* = 0.66$. The system is in a columnar state.

bution" to $\exp 6i\theta_{ij}$), but within one column, because of disorder, more than one particle can be within the cutoff distance $0.7r_{\parallel NN}$ of a neighboring particle and can thus contribute to the sum.

C. $L/D = 5$, 90 particles: results

1. MC results

For the 90-particle system at $L/D = 5$ both the run starting from the ABC-stacked lattice and the run starting from the columnar configuration showed similar behavior: the ABC-stacked lattice melted into a columnar-like structure at a density $\rho^* \approx 0.80$: at this density the ABC-like stacking was changed into an AAA-like stacking (Fig. 2). The longitudinal distribution function revealed, however, that the distribution of the particles in the parallel direction was not uniform: there was still a clear periodicity within the system, indicating that the structure is still crystalline. Upon further expansion, the structure became more and more uniform, with a small amount of periodicity still remaining (Fig. 3). Apparently the system needs much time (i.e., many MC cycles) to attain a columnar phase. The system melted into a smectic-A phase at a density $\rho^* \approx 0.60$.

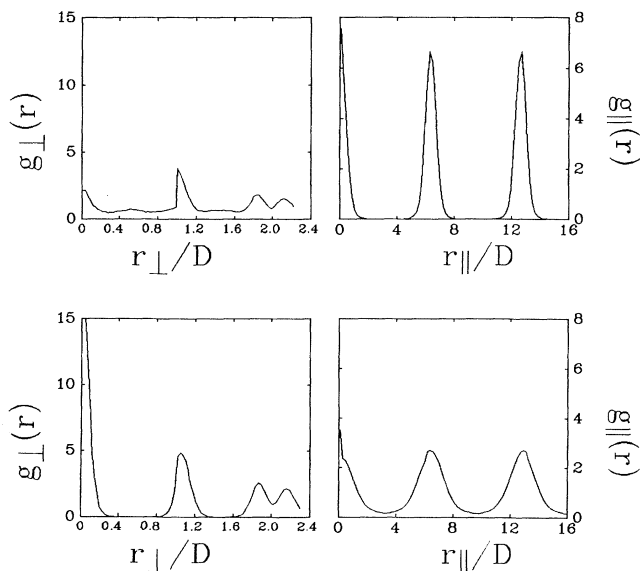In the expansion series starting from the columnar state (which by construction had no periodicity in the

FIG. 2. Transverse and longitudinal pair distribution functions for the $L/D = 5$, 90-particle system at densities $\rho^* = 0.82$ (top) and 0.78 (bottom). The configurations were obtained by expanding a solid phase. Note that at $\rho^* = 0.78$ a peak occurs in $g_\perp(r)$ at $r = 0$, indicating that the stacking is changed from "interstitial" to "top on top."
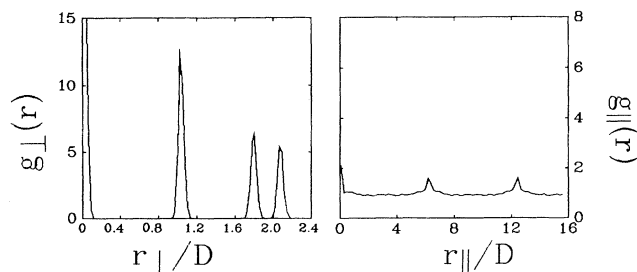

FIG. 4. Same as in Fig. 2 for $L/D = 5$, 90 particles at a density $\rho^* = 0.88$. This diagram is obtained when a columnar phase is compressed. The system is still in a columnar phase. The peaks are caused by the periodicity within a column.

parallel direction), the system initially showed an increase of the periodicity upon expansion, but then the results became comparable with the ones of the runs starting from the lattice.

We also performed a series of runs in which a columnar configuration was compressed. Here, the "columnarity" of the system became more and more pronounced (Fig. 4). $g_{\parallel}$ is very uniform at a density $\rho^* = 0.88$, with a few small peaks, which are caused by the periodic distribution of particles in the same column. This is in accordance with the results of Ref. 7, where the columnar phase was obtained by compression.

2. MD results

Figure 5 shows the typical time evolution of the quantities mentioned in Sec. II B at high densities (in this picture $\rho^* = 0.76$): the system is in a stable columnar phase $[\psi_6^2 > 1$, $S_m(\mathbf{k}_{\parallel})$ small, $S_m(\mathbf{k}_{\perp})$ large]. Note that the diffusion in the parallel direction (within the columns) is extremely large.

At lower densities ($\rho^* < 0.68$), solidlike fluctuations occur within the columnar phase, which extend throughout the entire system. Through snapshots the structure of such a fluctuation can be identified as that of an $A A A$-stacked lattice. At a density $\rho^* = 0.60$ the system has melted into a smectic-A phase.

D. 1080-particle systems: results

1. MC results

In the 1080-particle runs, results for runs starting from different configurations yielded distinct results. Expan-

sion of an ABC-stacked lattice showed the periodicity in the parallel direction to be nearly constant. Snapshots revealed in the $L/D = 5$ system an increasing tendency towards the $A A A$-like stacking below a density $\rho^* \approx 0.78$. For higher densities the original ABC stacking was stable. Runs starting from a columnar phase remained in this phase upon expansion, although an increase in $A A A$-like periodicity was observed when the density was decreased. The system melted into a smectic-A phase at $\rho^* \approx 0.60$ for all runs. Similar behavior was observed in the $L/D = \infty$ system.

From these results it is not possible to tell if the columnar phase is thermodynamically stable. More information can be gained from the MD simulations described below.

2. MD results

$L/D = 5$. Analysis of the simulation results for a system of 1080 particles over a range of densities from the fluid ($\rho^* = 0.20$) to a dense solid ($\rho^* = 0.86$) indicated that the columnar phase is nowhere mechanically stable.

For $\rho^* > 0.84$ the stable structure is the ABC-stacked lattice. For $0.74 \leq \rho^* \leq 0.84$ the system appears to be fluctuating between a state with a high value of $S_m(\mathbf{k}_{\perp})$, and one with a low value, while $\langle R_{\perp}^2(t) \rangle$ shows a small but steady diffusion. Snapshots reveal that the system is fluctuating between configuraitons with predominantly $A A A$-like stacking and ABC-like stacking. Another possible interpretation is that the phase should be identified as a smectic-B phase. During the fluctuations the compressibility factor remained constant, and we could not find hysteresis effects upon compression and subsequent expansion.

For $0.66 \leq \rho^* < 0.74$ the system is in a state with a high value of the structure factors in both directions: an $A A A$-stacked lattice. Figure 6 clearly shows the difference in stacking properties between an $A A A$- and an ABC-stacked lattice.

For $\rho^* < 0.66$ the system melts into a smectic-A phase. Note that this phase occurs at a higher density than in the 90-particle system,[7] where a columnar–smectic-A transition was observed.

$L/D = \infty$. In this system the $A A A$-stacked phase is stable for $0.64 \leq \rho^* \leq 0.78$. For $\rho^* < 0.64$ the system is in a smectic-A phase, for $\rho^* > 0.78$ the system appears to prefer a columnar state, irrespective of the starting configuration. When we performed a run on a columnar phase with 2160 particles and 18 layers in the parallel direction at $\rho^* = 0.82$, however, the system evolved towards an $A A A$-stacked phase again. Obviously here too, the stability of the columnar phase depends strongly on system size. One may wonder whether a stable columnar phase will exist at high densities in a macroscopic system. On the basis of our present data we cannot answer this question. A systematic study using much larger systems would be needed to answer it.

E. Discussion

From the results presented above we are able to draw a number of conclusions. First, the columnar state, that
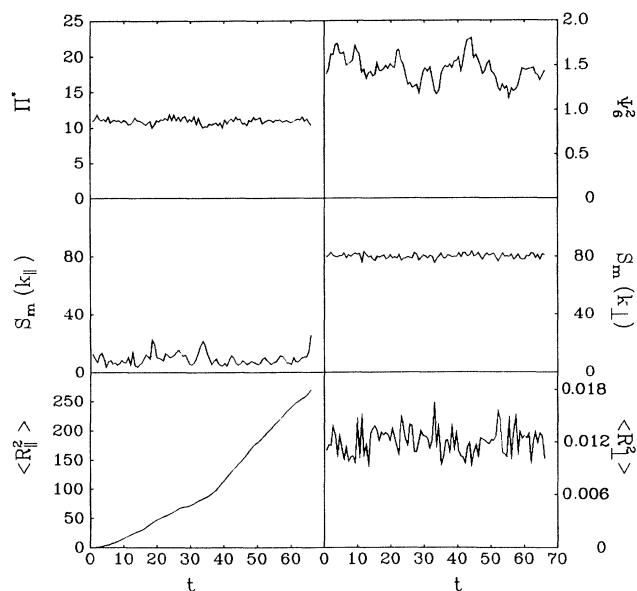

FIG. 5. Time evolution of the $L/D = 5$, 90-particle system at $\rho^* = 0.76$. The system is in a stable columnar phase with a large rate of diffusion in the parallel direction.

was found to be a stable phase in the 90-particle system, is replaced by a hexagonal crystalline phase as the system size is increased. Obviously, the small system size allows an unphysical diffusion. This effect does not only occur in the parallel direction, as is demonstrated by the following experiment (Fig. 7): in the $L/D = 5$ system we started from a columnar configuration of 1080 particles at $\rho^* = 0.80$ where each column had 36 particles. The system was therefore small in the transverse direction. As can be seen from ψ_6^2 and $S_m(\mathbf{k}_\parallel)$ the system becomes periodic in the parallel direction (an $A A A$-stacked lattice). When this has happened, however, $S_m(\mathbf{k}_\perp)$ becomes zero quickly, and there is an onset of diffusion in the transverse direction, while the bond order remains intact. The interpretation is that now there is an unphysical diffusion of hexagonally stacked layers in the transverse
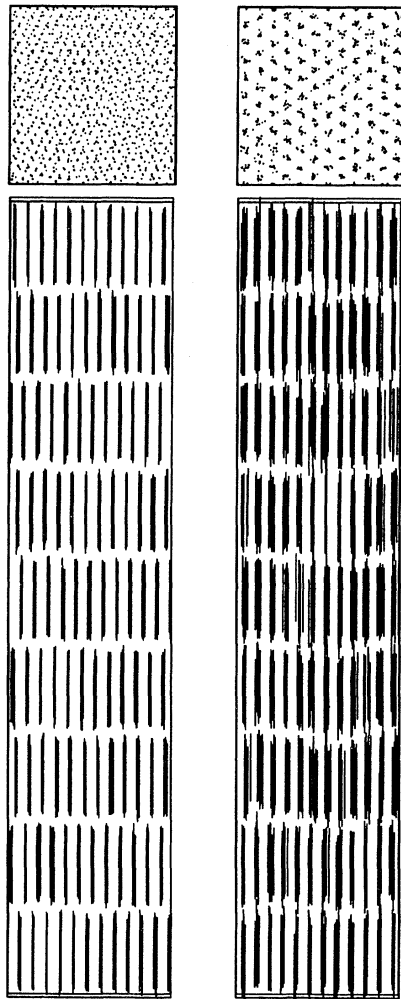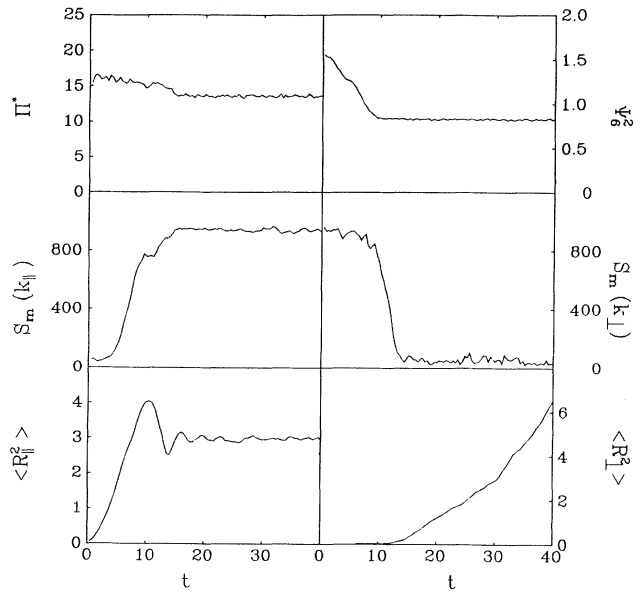

FIG. 7. Time evolution for a $L/D = 5$, 1080-particle system with 36 layers in the parallel direction at $\rho = 0.80$. The system starts from a columnar configuration. First it evolves into a solid phase, but then the solid layers begin to diffuse in the transverse direction. This diffusion is an artifact of the small system size in the transverse direction.

direction. The conclusion we can draw from this is that the system size should be large in all directions to prevent the onset of unphysical diffusion.

In the smectic-A phase the particle positions within the layers are not correlated over large distances. In that case the diffusion within the layers is not sensitive to the
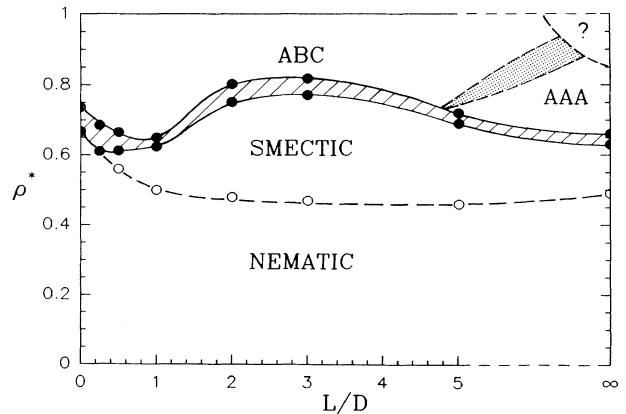

FIG. 6. Stable solid structures at $\rho^* = 0.82$ (left) and $\rho = 0.70$ (right). The particles are represented by lines of length L. Top pictures: top view. Bottom pictures: side view. (All pictures show projections.) The difference between ABC and $A A A$ stacking is clearly visible.

FIG. 8. Revised phase diagram for the spherocylinder system (compare with Fig. 1). The $A A A$-ABC transition point could not be determined, but lies somewhere within the dotted region. The question mark indicates that within the area bounded by the dashed line, our results give no conclusive evidence about which phase is stable.

boundary conditions. Unlike the columnar phase, the range of stability of the smectic-A phase does not depend significantly on system size.

The question remains if parallel spherocylinders with $L/D = \infty$ have a "pocket" in the phase diagram where the columnar phase is stable. As remarked above, for the $L/D = \infty$ system a columnar phase is still observed for $\rho^* > 0.78$, but it turns out to be unstable at $\rho^* = 0.82$ when the system size is doubled in the parallel direction. On the basis of our simulation results we cannot tell what happens to this columnar phase in the thermodynamic limit. The present simulations suggest that no stable columnar phase exists as $N \to \infty$. It is, however, conceivable that over much larger distances than those studied in this work the correlation in the z coordinates of the particles in an AAA-stacked system disappears, so that macroscopically the phase is columnar. The mechanism underlying this columnarity would, however, be fundamentally different from the one that is responsible for the stability of the columnar phase in small systems.

A columnar phase has also been observed in simulations of a system of cut spheres.[5] The columnar phase in this system is, however, fundamentally different from the one observed in the spherocylinder system: in the cut-sphere phase, the columnarity occurs because there is no correlation in particle positions over large distances, neither for particles of different columns nor for particles within a column. This phase is stable for large system sizes. In the spherocylinder phase the particle positions *within* a column are strongly correlated over the whole box range. Here the columnarity occurs because particle positions in *different* columns are not correlated, because of the strong (unphysical) diffusion of entire columns.

As mentioned in the Introduction, some theories predict that parallel spherocylinders have a stable columnar phase. However, this discrepancy between theory and experiment may not be as serious as it seems. A possible
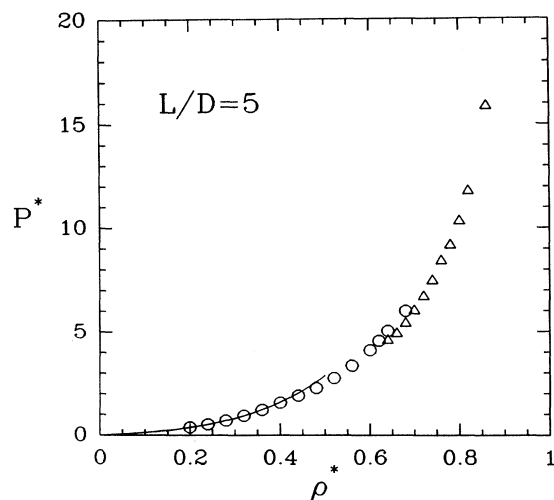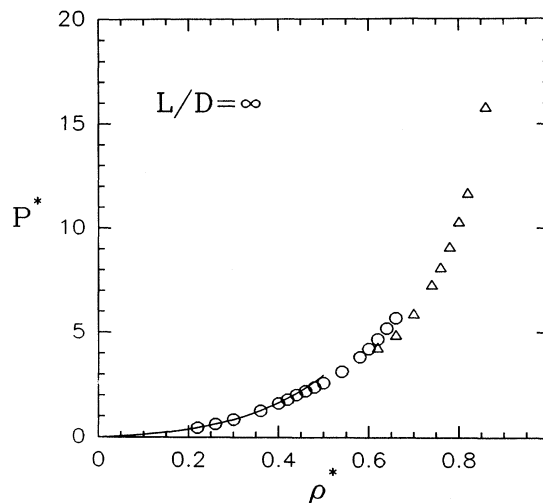

FIG. 10. Equation of state for the $L/D = \infty$, 1080-particle sytem. Circles: nematic and smectic branches. Triangles: solid branch.

explanation for the stability of the columnar phase in Ref. 11 is that in their model, Taylor, Hentschke, and Herzfeld did not take the interaction between the columns into account. Such an interaction is apparently responsible for the preference of the system for the AAA-stacked phase. In Ref. 13 the columnar phase is indeed found to be unstable with respect to solidlike fluctuations, although the wave vector at which the divergence occurs is not compatible with an AAA-stacked phase. In Ref. 14 the columnar phase was found to be unstable by a direct analysis. Below we compare our results for the various phase-transition densities with these theories.

FIG. 9. Equation of state for the $L/D = 5$, 1080-particle system. Circles: nematic and smectic branches. Triangles: solid branch.

TABLE I. Equation of state for the various phases in the $L/D = 5$ system. Numbers in parentheses represent uncertainty figures.

Liquid crystal		Solid	
ρ^*	Pv_0/kT	ρ^*	Pv_0/kT
0.20	0.371(1)	0.64	4.586(68)
0.24	0.521(2)	0.66	4.910(17)
0.28	0.704(4)	0.68	5.407(36)
0.32	0.941(3)	0.70	6.017(11)
0.36	1.223(7)	0.72	6.692(25)
0.40	1.570(14)	0.74	7.449(31)
0.44	1.915(12)	0.76	8.407(54)
0.48	2.279(10)	0.78	9.149(19)
0.52	2.758(33)	0.80	10.312(59)
0.56	3.363(12)	0.82	11.762(20)
0.60	4.114(16)	0.86	15.849(35)
0.62	4.569(16)		
0.64	5.054(17)		
0.68	6.013(34)		

III. REVISION OF THE PHASE DIAGRAM

Figure 8 shows the revised phase diagram of a system of parallel hard spherocylinders. Below we describe the free-energy calculations that allow us to estimate the range of thermodynamic stability of the various phases in the 1080-particle system.

A. Equation of state

Figures 9 and 10 and Tables I and II give the equation of state for the $L/D = 5$ and ∞ systems, respectively. The data were obtained by performing MD simulations on equilibrated configurations. Our values are comparable with those of Ref. 7 for the nematic and smectic-A phases for densities $\rho^* \leq 0.60$.

Note that for both values of L/D there is a first-order transition between the smectic-A and the solid phase. In the $L/D = 5$ system the transition between the AAA-stacked and ABC-stacked solids does not show in the equation of state.

B. Nematic–smectic-A transition

We estimated the position of the nematic–smectic-A transition by studying the critical slowing down of the intermediate scattering function $F(k_z, t)$ (Ref. 16) defined by

$$F(k_z, t) = \langle \rho(k_z, 0)\rho(-k_z, t) \rangle \ . \tag{8}$$

Figures 11 and 12 show the relaxation rates of $F(k_z, t)$ as a function of density for $L/D = 5$ and ∞, respectively. From these data we inferred the transition densities for the nematic–smectic-A transition (Table III). In Ref. 7, for $L/D = \infty$, the same transition was estimated from the behavior of the static structure factor. The latter method is less accurate and results in a somewhat lower estimate for the transition density. The estimate for the

FIG. 11. Relaxation rate of $F(k_z, t)$ [Eq. (8)] for the $L/D = 5$, 1080-particle system.

nematic–smectic-A transition for $L/D = 5$ was in both cases obtained from dynamical measurements, and gives identical results, independent of the system size. In Ref. 14 the nematic–smectic-A phase is predicted to occur at $\rho^* = 0.31$ for $L/D = \infty$, which is somewhat lower than our simulation results.

C. Smectic-A–hexagonal transition

1. Technical details

We determined the transition densities by using the standard techniques described in previous articles.[6,7] Below we give a brief summary of these techniques.

The transition densities are given by the densities for which

$$P_{\mathrm{I}} = P_{\mathrm{II}} \ , \quad G_{\mathrm{I}} = G_{\mathrm{II}} \ , \tag{9}$$

where G is the Gibbs free energy defined by

$$G = F + PV \ . \tag{10}$$

In order to determine the transition densities, both the pressure and the free energy of the phases have to be known. The pressure is directly obtained from the MD simulations. The Helmholtz free energy per particle can be determined by the following equation:

$$f - f_0 = \int_{\rho_0}^{\rho} P(\rho')/(\rho')^2 d\rho' \ . \tag{11}$$

TABLE II. Equation of state for the various phases in the $L/D = \infty$ system. Numbers in parentheses represent uncertainty figures.

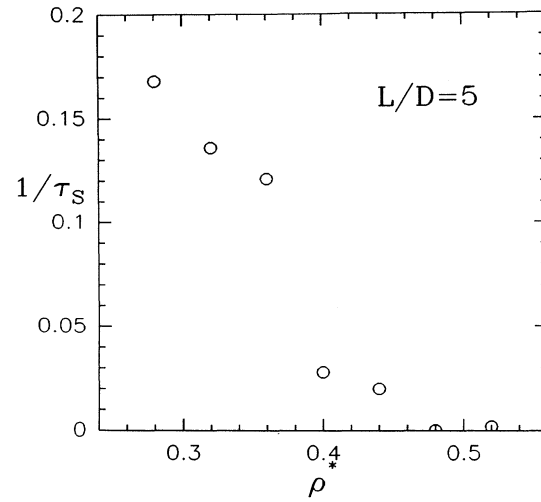| Liquid crystal		Solid	
ρ^*	Pv_0/kT	ρ^*	Pv_0/kT
0.22	0.457(2)	0.62	4.218(71)
0.26	0.630(2)	0.66	4.830(13)
0.30	0.848(4)	0.70	5.846(7)
0.36	1.268(8)	0.74	7.228(10)
0.40	1.621(10)	0.76	8.063(24)
0.42	1.802(11)	0.78	9.045(33)
0.44	2.034(7)	0.80	10.241(52)
0.46	2.215(8)	0.82	11.619(16)
0.48	2.396(10)	0.86	15.751(23)
0.50	2.596(10)		
0.54	3.136(17)		
0.58	3.832(9)		
0.60	4.221(60)		
0.62	4.678(16)		
0.64	5.195(13)		
0.66	5.689(34)		

TABLE III. Nematic–smectic-A transition densities as determined by the relaxation times of $F(k_z, t)$. The results of the 90-particle system (Ref. 7) are also given.

	1080 particles	90 particles
$L/D = 5$	0.46	0.46
$L/D = \infty$	0.49	0.39

TABLE IV. Free energy of the smectic phase f_c at a density ρ_c^*, and free energy of the solid phase f_0, at a density ρ_0^∞. Numbers in parentheses represent uncertainty figures.

L/D	ρ_c^*	f_c	ρ_0^*	f_0
5	0.40	−1.239	0.70	2.510(35)
∞	0.40	0.570	0.70	4.220(22)

f_0 is the Helmholtz free energy at density ρ_0.

For the smectic-A phase the excess Helmholtz free energy can be determined by using the property that the system behaves as an ideal gas at zero density. The free energy of the AAA-stacked phase was calculated by thermodynamic integration to an Einstein crystal with an AAA-stacked structure.[17]

Once the absolute free energy of both phases is known at one density, it is known for all densities where the phase is mechanically stable through Eq. (11). The integration in Eq. (11) was performed by fitting the pressure to a y expansion:[18]

$$P^*(\rho) = \sum_n C_n^* y^n , \qquad (12)$$

where $P^* = P v_0 / kT$, with v_0 the volume of a particle, and

$$y = \frac{v_0 \rho}{1 - v_0 \rho} . \qquad (13)$$

Finally, the transition densities are determined by applying Eqs. (9).

2. Results

In Table IV the absolute free energies for the smectic-A phase and the AAA-stacked solid are given, determined in the way indicated in Sec. III C 1, and together with the densities at which they were calculated. For the calculation of the free energy of the smectic-A phase we made use of the virial coefficients given in Ref. 7.

The C_n coefficients for the pressure in the y expansion [Eq. (12)] are given in Table V. Finally, the transition densities are given in Table VI. Not surprisingly, the transitions occur at densities that are considerably higher than the smectic-A–columnar transition densities that are found in the 90-particle system.[7] Reference 14 predicts the transition in the $L/D = \infty$ system to occur at $\rho^* = 0.59$, which is again somewhat lower than our result.

FIG. 12. Relaxation rate of $F(k_z, t)$ for the $L/D = \infty$, 1080-particle system.

D. Hexagonal-ABC transition

As mentioned above, the $L/D = 5$ system is seen to fluctuate between ABC-like and AAA-like stacking for $0.74 \leq \rho^* \leq 0.82$. During these fluctuations the pressure remains constant. This suggests that there is a continuous or weakly first-order transition between the hexagonal phase and the ABC-stacked phase.

IV. SUMMARY

We have shown that the columnar phase that occurs in small systems of parallel hard spherocylinders transforms into a hexagonal crystalline phase when the system size is increased. The mechanism stabilizing the columnar phase in the 90-particle system appears to be the strong alignment of particles within a column, which, because of the finite system size and the periodic boundary conditions, allows the columns to slide as a whole. We determined the transition densities between the various phases. A revised phase diagram is given in Fig. 8.

No significant system size dependence was observed for the smectic phase. Finally, it should be noted that the columnar phase observed in freely rotating cut spheres is of a different nature than that found for similar systems

TABLE V. Coefficients for the y-expansion fits to the equation-of-state data. Column 3 gives the range of validity of the expansion.

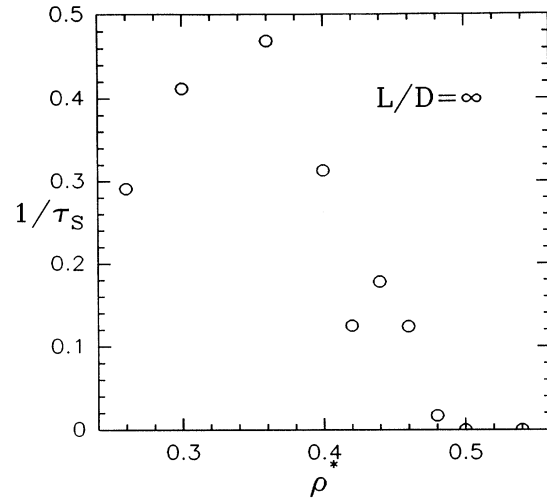| L/D	Phase	ρ^*	C_1^*	C_2^*	C_3^*	C_4^*
5	Smectic	0.40–0.70	1.845	2.002	−0.352	
	Solid	0.64–0.86	1.102	2.834	−1.017	0.162
∞	Smectic	0.40–0.66	2.440	0.790	0.110	
	Solid	0.62–0.76	2.627	0.346	0.046	

TABLE VI. Transition densities for smectic-solid transition for $N=1080$ particles, and smectic-columnar transition for $N=90$ particles. The 90-particle data are taken from Ref. 7. Numbers in parentheses represent uncertainty figures.

L/D	N	ρ_{sm}^*	ρ_{so}^*	ρ_{co}^*
5	1080	0.69(3)	0.72(3)	
	90	0.613		0.694
∞	1080	0.63(1)	0.66(1)	
	90	0.56		0.56

of parallel spherocylinders; in particular, stable columnar phases of cut spheres are also found in large systems.

ACKNOWLEDGMENTS

APPENDIX

As remarked in Sec. II B, the wave vectors for which the maximum value of the structure factors is determined are bounded by a cutoff. In this appendix we discuss how the cutoff was defined.

For wave vectors parallel to the alignment of the cylinders (i.e., the z direction), this cutoff is

$$1 \le \frac{k_z B_z}{2\pi} \le 128 . \tag{A1}$$

Here B_x is the length of the simulation box in the z direction. For wave vectors perpendicular to the alignment of the cylinders, we used as a cutoff

$$2 \le \left[\frac{k_x B_x}{2\pi}\right]^2 + \left[\frac{k_y B_y}{2\pi}\right]^2 \le 144 . \tag{A2}$$

Here B_x and B_y are the dimensions of the box in the x and y directions, respectively. The wave vectors for which the maxima occur were also recorded. $S_m(\mathbf{k}_\parallel)$ can be used to discern a columnar phase from a solid or smectic phase. The interpretation of $S_m(\mathbf{k}_\perp)$ is dependent on

the system size: define N_x, N_y to be the number of Bravais unit cells of an ABC-stacked lattice in the x and y directions, respectively, corresponding to the box size and density in the system. Define

$$(\xi_x, \xi_y) \equiv \left[\frac{x}{B_x}, \frac{y}{B_y}\right] , \quad (\kappa_x, \kappa_y) \equiv \left[\frac{k_x B_x}{2\pi}, \frac{k_y B_y}{2\pi}\right] , \tag{A3}$$

then the coordinates of the particles in an ABC-stacked lattice are given by

$$(\xi_x, \xi_y) = \left[\frac{n + \frac{1}{2}l}{N_x}, \frac{l}{6N_y}\right] ,$$

$$-3N_y \le l \le 3N_y , \quad -\tfrac{1}{2}N_x \le n + \tfrac{1}{2}l \le \tfrac{1}{2}N_x \tag{A4}$$

(we chose the ξ coordinates to be between $-\frac{1}{2}$ and $\frac{1}{2}$). In the AAA-stacked lattice the coordinates are given by

$$(\xi_x, \xi_y) = \left[\frac{n + \frac{1}{2}l}{N_x}, \frac{l}{2N_y}\right] ,$$

$$-N_y \le l \le N_y, -\tfrac{1}{2}N_x \le n + \tfrac{1}{2}l \le \tfrac{1}{2}N_x . \tag{A5}$$

In our 90-particle system $(N_x, N_y) = (5,3)$. Therefore the wave vectors that give a nonvanishing contribution to the structure factor are

$$(\kappa_x, \kappa_y) = (0, \pm 6), (0, \pm 12), (\pm 5, \pm 3), (\pm 5, \pm 9) \tag{A6}$$

for the AAA lattice, and

$$(\kappa_x, \kappa_y) = (\pm 5, \pm 9) \tag{A7}$$

for the ABC lattice. In the 1080-particle system $(N_x, N_y) = (10,6)$. Now the contributing wave vectors are

$$(\kappa_x, \kappa_y) = (0, \pm 12), (\pm 10, \pm 6) \tag{A8}$$

for the AAA lattice, and there are no contributing wave vectors for the ABC lattice. Therefore, in the 90-particle system $S_m(\mathbf{k}_\perp)$ remains high both for the AAA and ABC lattices, but an identification of both lattice types remains possible through the wave vectors for which the maximum value is obtained. In the 1080-particle system $S_m(\mathbf{k}_\perp)$ is larger for an AAA-stacked lattice and a columnar phase, but small for an ABC-stacked lattice and a smectic phase. This is of course an artifact of the cutoff, but it facilitates the identification of the AAA- and ABC-stacked phases.

[1]D. Frenkel and B. M. Mulder, Mol. Phys. **55**, 1171 (1985).

[2]R. Eppenga and D. Frenkel, Mol. Phys. **52**, 1303 (1984).

[3]J. Vieillard-Baron, Mol. Phys. **28**, 809 (1974).

[4]D. Frenkel, H. N. W. Lekkerkerker, and A. Stroobants, Nature **332**, 882 (1988).

[5]D. Frenkel, Liquid Cryst. **5**, 929 (1989).

[6]J. A. C. Veerman and D. Frenkel, Phys. Rev. A **41**, 3237

(1990).

[7]A. Stroobants, H. N. W. Lekkerkerker, and D. Frenkel, Phys. Rev. A **36**, 2929 (1987).

[8]B. Mulder, Phys. Rev. A **35**, 3095 (1987).

[9]R. Hołyst and A. Poniewierski, Phys. Rev. A **39**, 2742 (1989).

[10]X. Wen and R. B. Meyer, Phys. Rev. Lett. **59**, 1325 (1987).

[11]M. P. Taylor, R. Hentschke, and J. Herzfeld, Phys. Rev. Lett.

62, 800 (1989).

[12]J. M. Caillol and J. J. Weis, J. Chem. Phys. **90**, 7403 (1989).

[13]A. M. Somoza and P. Tarazona, Phys. Rev. A **40**, 4161 (1989).

[14]R. Hołyst and A. Poniewierski, Mol. Phys. (to be published).

[15]J. A. C. Veerman and D. Frenkel, Physica A **156**, 599 (1989).

[16]D. Frenkel, Mol. Phys. **60**, 1 (1987).

[17]D. Frenkel and A. J. C. Ladd, J. Chem. Phys. **81**, 3188 (1984).

[18]B. Barboy and W. M. Gelbart, J. Chem. Phys. **71**, 3053 (1979).